DALTON

Synthesis, structure and polarized optical spectroscopy of two new fluoromanganese(III) complexes †

Pedro Núñez,*[a] Carlos Elías,[a] Jesús Fuentes,[a] Xavier Solans,[b] Alain Tressaud,[c] M. Carmen Marco de Lucas[d] and Fernando Rodríguez[d]

[a] *Departamento de Química Inorgánica, Universidad de La Laguna, 38200 La Laguna, Tenerife, Spain*
[b] *Departament de Cristallografia, Mineralogia i Dipòsits Minerals, Universitat de Barcelona, 08028 Barcelona, Spain*
[c] *ICMCB, Universitè de Bordeaux I, Av. Dr. Shweitzer, 33608, Pessac, France*
[d] *Departamento de Ciencias de la Tierra y Física de la Materia Condensada, Facultad de Ciencias, Universidad de Cantabria, 39005 Santander, Spain*

The syntheses and crystal structures of two new fluoromanganese(III) complexes are reported; $[MnF_3(H_2O)(2,2'\text{-bipy})]$ **1** and 4,4′-bipy$H_2[MnF_4(H_2O)_2]\cdot 2H_2O$ **2**, where 2,2′-bipy and 4,4′-bipy are 2,2′-bipyridyl and 4,4′-bipyridyl, respectively. Compound **1**: monoclinic, space group $P2_1/n$, $a = 1973.7(4)$, $b = 749.0(2)$, $c = 903.1(3)$ pm, $\beta = 95.22(3)°$, $Z = 4$, $R1 = 0.051$. Compound **2**: monoclinic, space group $P2_1$, $a = 516.4(2)$, $b = 1851.9(4)$, $c = 986.3(3)$ pm, $\beta = 99.07(2)°$, $Z = 2$, $R1 = 0.028$. The manganese co-ordination environment was found to be octahedral in both compounds, but strongly distorted by the Jahn–Teller effect as a result of the high-spin d^4 configuration of Mn^{3+}. A very extensive intermolecular hydrogen-bond framework is present in both compounds. For compound **1** the octahedra are linked through hydrogen bridges resulting in octahedral manganese chains. For compound **2**, the octahedra $[MnF_4(H_2O)_2]^-$ are associated *via* hydrogen bonds into chains, which in turn are connected by interchain hydrogen bridges. The polarized optical spectra of single crystals are presented and explained in terms of intraconfigurational d^4 transitions split by ligand fields of nearly C_s and D_{4h} symmetries for compounds **1** and **2**, respectively. The results are compared with those available for other Mn^{III} fluorides.

Manganese(III) compounds are attractive systems for studying optical properties associated with Jahn–Teller distortions. In particular the study of the polarized optical spectra is important since the corresponding crystal field electronic transitions are responsible for both the color and the strong dichroism exhibited by some Mn^{III} crystals. Owing to this, spectroscopic studies yielding correlations between the local structure of the Mn^{III} complex and its electronic spectra are worthwhile in order to establish guidelines to be followed for the synthesis of Mn^{III}-based optical materials. Interestingly, this kind of structural correlation has never been made in heteroligand complexes of Mn^{III}.

We have observed a large variety of structural, magnetic and optical behaviors during the investigation carried out on fluoromanganese(III) complexes containing inorganic counter ions.[1–7] It is well established that Mn^{III} has a strong tendency to form highly distorted $[MnF_6]^{3-}$ octahedra due to the Jahn–Teller effect, which arises from the high-spin d^4 configuration of Mn^{III}.[8,9] These distorted octahedra can be isolated or linked in one-, two- or three-dimensions, depending on the nature of the counter ion.

The substitution of the inorganic cations by nitrogen-containing organic bases in the fluoromanganate lattices is expected to lead to the formation of octahedral chains or layers, which should be farther apart from one another due to the larger size of the organic bases relative to the inorganic cations. These types of compounds would be good candidates for modeling one- or two-dimensional interactions, since the perturbations arising from interchain or interlayer interactions would be minimized. For this reason, we have been interested in coupling fluoromanganese(III) complexes with organic bases, which is the aim of this paper. A similar substitution was reported in a recent paper describing the synthesis and structure of $enH_2[MnF_5]$ (enH_2 = ethylenediammonium),[10] resulting in a one-dimensional structural arrangement. Organic-base chloromanganese(III),[11] organic-base fluoromanganese(III)[12] and related fluoromanganese(III)[13] complexes were described some time ago, but no crystal data are available for them. Among these manganese(III) complexes, it is worthwhile to mention $[MnF_3(H_2O)(2,2'\text{-bipy})]\cdot 2H_2O$ (2,2′-bipy = 2,2′-bipyridyl) which although similar to compound **1** described below, incorporates two extra water molecules.

In this paper we describe the structures and polarized optical spectra of two new fluorocomplexes of manganese(III): aqua(2,2′-bipyridine)trifluoromanganese(III) $[MnF_3(H_2O)(2,2'\text{-bipy})]$, and 4,4′-bipyridinediium bis[diaquatetrafluoromanganese(III)] 4,4′-bipy$H_2[MnF_4(H_2O)_2]\cdot 2H_2O$ **2** (4,4′-bipy = 4,4′-bipyridyl).

Experimental

Preparation of compounds

Manganese(III) oxide was prepared as described elsewhere[14] and checked by powder X-ray diffraction, 2,2′-bipy and 4,4′-bipy (Aldrich) were used without further purification.

The complexes $[MnF_3(H_2O)(2,2'\text{-bipy})]$ and 4,4′-bipy$H_2[MnF_4(H_2O)_2]\cdot 2H_2O$ were prepared by dissolving Mn_2O_3 (0.79 g, 5 mmol) in hot 48% HF (20 ml), to which a solution of 2,2′-bipy or 4,4′-bipy (1.56 g, 10 mmol) in 2% HF (20 ml) was added. **CAUTION!!** *Due to its high toxicity and reactivity, any manipulation with hydrofluoric acid must be carried out in Teflon or other suitable plastic ware in a well ventilated hood.* Large crystals could be obtained by slow vapor–liquid diffusion of ethanol into the resulting solution at about 5 °C. The crystals of $[MnF_3(H_2O)(2,2'\text{-bipy})]$ **1** are dark purple in color and approximately plate shaped, while the crystals of 4,4′-

† *Non-SI unit employed*: $\mu_B \approx 9.274 \times 10^{-24}$ J T^{-1}.

bipyH_2[$MnF_4(H_2O)_2$]·$2H_2O$ **2** consisted of long brownish red needles, which however were generally twinned. Under polarizing microscope, crystals of compound **1** exhibit an intense dichroism in the (001) plane. The crystal color changes from red to yellow-green when electrical field E changes from the b to the a axis. For compound **2** the available needle-like crystals displayed only very weak dichroism. The crystals used in the spectroscopic measurements were previously oriented on a four-circle diffractometer.

Collection and reduction of X-ray data

Compound 1. $C_{10}H_{10}F_3MnN_2O$, $M = 286.14$, monoclinic, $a = 1973.7(4)$, $b = 749.0(2)$, $c = 903.1(3)$ pm, $\beta = 95.22(3)°$, $U = 1329.5(6) \times 10^{-30}$ m^3 (by least-squares refinement on diffactometer angles from 25 centered reflections, $12 \leqslant \theta \leqslant 16°$), $T = 293$ K, space group $P2_1/n$ (no. 14), graphite-monochromated Mo-Kα radiation, $\lambda = 71.069$ pm, $Z = 4$, $D_c = 1.430$ Mg m^{-3}, $F(000) = 576$, dark purple prism with dimensions $0.1 \times 0.2 \times 0.1$ mm, μ(Mo-Kα) = 1.013 mm^{-1}, no absorption correction, Philips PW-1100 diffactometer, ω–2θ scans, data collection range $2.91 \leqslant \theta \leqslant 29.96°$, $-27 \leqslant h \leqslant 27$, $0 \leqslant k \leqslant 10$, $0 \leqslant l \leqslant 12$, three standard reflections monitored every 3 h with no significant variation in intensity; 3538 reflections measured, 3356 unique ($R_{int} = 0.0125$) which were used in all calculations.

Compound 2. $C_{10}H_{22}F_8Mn_2N_2O_6$, $M = 528.18$, monoclinic, $a = 516.4(2)$, $b = 1851.9(4)$, $c = 986.3(3)$ pm, $\beta = 99.07(2)°$, $U = 931.4(5) \times 10^{-30}$ m^3 (by least-squares refinement on diffractometer angles from 24 centered reflections, $12 \leqslant \theta \leqslant 21°$), $T = 293$ K, space group $P2_1$ (no. 4), graphite-monochromated Mo-Kα radiation, $\lambda = 71.069$ pm, $Z = 2$, $D_c = 1.883$ Mg m^{-3}, $F(000) = 532$, brownish red needle with dimension $0.2 \times 0.1 \times 0.05$ mm, μ(Mo-Kα) = 1.463 mm^{-1}, no absorption corrections, Enraf-Nonius diffractometer, data collection range $2.09 \leqslant \theta \leqslant 29.97°$, $-7 \leqslant h \leqslant 7$, $0 \leqslant k \leqslant 26$, $0 \leqslant l \leqslant 13$, three standard reflections monitored every 3 h with no significant variation in intensity; 2918 reflections measured, 2788 unique ($R_{int} = 0.0273$) which were used in all calculations.

Refinement of structures. Neutral atomic scattering factors as well as absorption coefficients were taken from ref. 15. The initial structural solutions were obtained by interpreting Patterson maps, using the SHELXS computer program.[16] Heavy atoms not located from the initial structure solution were found by successive Fourier or Fourier-difference maps with intervening cycles of least-squares refinement using the SHELXL 93 computer program.[17] All non-hydrogen atoms were treated anisotropically and refined by the full-matrix least-squares method. Although most aromatic hydrogen atoms could be located from the difference maps, they were placed using a 'riding' model and refined with an overall thermal parameter for each aromatic ring. In **1** the initial refinement indicated the presence of four co-ordinated fluorine atoms; however, this did not agree with the observed dichroism, which should be attributable to the presence of manganese(III). It was therefore assumed that in place of one of the fluorine atoms a water molecule was co-ordinated to the manganese. The presence of a water molecule was confirmed by the IR spectrum, which displayed a broad, intense peak at 3450 cm^{-1}. This peak is due to the presence of strongly hydrogen-bonded water molecules. In order to check the correct position of the water molecule around the manganese, bond valence calculations were carried out. The bond valence method allows one to check crystalline structures in a simple and elegant way. In particular, this method[18] is useful for verifying oxidation states and for distinguishing between ligands such as O^{2-}, OH^-, F^-, *etc.* Using the bond valence parameters R_{ij} (Å)[18] 1.66 (Mn–F), 1.760 (Mn–O) and 1.87 (Mn–N) the following values were obtained for the manganese valence in **1** 3.15 and **2** 3.05 [Mn(1)] and 3.10 [Mn(2)]. Using these values the nitrogen, oxygen and fluorine crystallographic positions were confirmed. These calculations were consistent with only one position for the water molecule. It was not, however, possible to locate the hydrogen atoms of this water molecule co-ordinated to the manganese. In **2**, all but one hydrogen [H(62)] belonging to water molecules were located and refined with an overall isotropic thermal parameter.

Table 1 Selected bond lengths (pm) and angles (°) for complexes **1** and **2**

Complex **1**			
Mn–F(1)	183.86(14)	Mn–F(2)	183.5(2)
Mn–F(3)	183.5(2)	Mn–O(1)	216.5(2)
Mn–N(1)	221.5(2)	Mn–N(2)	207.5(2)
N(1)–C(1)	131.4(3)	N(1)–C(5)	132.8(3)
N(2)–C(6)	133.6(3)	N(2)–C(10)	135.5(3)
F(3)–Mn–F(1)	176.53(7)	F(2)–Mn–N(2)	169.80(9)
O(1)–Mn–N(1)	169.59(8)	N(1)–Mn–N(2)	75.95(8)
C(1)–N(1)–C(5)	119.3(2)	C(6)–N(2)–C(10)	119.1(2)
Complex **2**			
Octahedron type A			
Mn(1)–F(1)	185.5(2)	Mn(1)–F(2)	181.7(2)
Mn(1)–F(3)	184.2(2)	Mn(1)–F(4)	184.4(2)
Mn(1)–O(1)	219.6(2)	Mn(1)–O(2)	223.8(2)
F(1)–Mn(1)–F(2)	178.1(1)	F(3)–Mn(1)–F(4)	177.98(8)
O(1)–Mn(1)–O(2)	178.0(1)		
Octahedron type B			
Mn(2)–F(5)	182.4(2)	Mn(2)–F(6)	186.2(2)
Mn(2)–F(7)	182.7(2)	Mn(2)–F(8)	179.6(2)
Mn(2)–O(3)	226.3(2)	Mn(2)–O(4)	220.0(2)
F(5)–Mn(2)–F(6)	178.3(1)	F(7)–Mn(2)–F(8)	179.8(1)
O(3)–Mn(2)–O(4)	177.2(1)		
Rings			
N(1)–C(3)	133.4(5)	N(1)–C(4)	132.9(4)
N(2)–C(8)	134.0(4)	N(2)–C(9)	132.8(5)
C(4)–N(1)–C(3)	122.2(3)	C(9)–N(2)–C(8)	121.9(3)

For compound **1**, the final $wR2(F^2)$ was 0.154 with conventional $R1(F)$ 0.0509, for 155 parameters and 0 restraints, $S = 0.993$, maximum $\Delta/\sigma = -0.007$, maximum $\Delta\rho = 1.835$ e Å^{-3}. For compound **2**, the final $wR2(F^2)$ was 0.0737 with conventional $R1(F)$ 0.0275, for 288 parameters and 1 restraint, $S = 1.010$, maximum $\Delta/\sigma = 0.077$, maximum $\Delta\rho = 0.657$ e Å^{-3}. The R factors were calculated as described elsewhere.[17] Selected bond distances for compounds **1** and **2** can be found in Table 1 and hydrogen bond distances in Table 2.

CCDC reference number 186/693.

Other physical measurements

The CHN analyses were obtained using a Carlo Erba EA-1108 automatic analyzer. The manganese(III) content was determined by back titration: a Fe^{II} solution (0.1 M) was added as a reducing agent to the aqueous solution containing the Mn^{III} sample. The excess Fe^{II} was titrated with a standard $K_2Cr_2O_7$ solution (0.0167 M) using sodium diphenylamine-4-sulfonate (0.2% ethanolic solution) as an indicator. Compound **1**, Found (Calc): C, 37.29 (37.09); H, 3.88 (4.49); Mn, 19.0 (19.20); N, 8.57 (8.89)%. Compound **2**, Found (Calc): C, 23.02 (22.74); H, 4.26 (4.20); Mn, 20.6 (20.8); N, 5.32 (5.30)%.

A Lambda 9 Perkin-Elmer spectrophotometer equipped with Glan Taylor polarizing prisms was employed for recording the polarized optical absorption spectra. Infrared spectra were carried out using KBr pellets on a Nicolet Fourier-transform infrared spectrophotometer. IR spectra (cm^{-1}): 3450s (br), 1654m,

Table 2 Hydrogen bond lengths (pm) for complexes **1** and **2**

Complex **1**			
$O(1)\cdots F(1)^{a}$	263.3(3)	$O(1)\cdots F(3)^{b}$	264.9(3)
Complex **2**			
Intrachain hydrogen bonds			
$F(3)\cdots O(2)^{c}$	267.7(3)	$F(4)\cdots O(1)^{d}$	271.4(3)
$F(5)\cdots O(4)^{d}$	266.6(4)	$F(6)\cdots O(3)^{c}$	274.0(3)
Interchain hydrogen bonds			
$F(1)\cdots O(4)$	270.8(3)	$F(4)\cdots O(3)^{e}$	277.7(3)
$F(7)\cdots O(1)^{f}$	260.9(4)	$F(8)\cdots O(2)$	293.8(4)
Other hydrogen bonds			
$F(1)\cdots O(6)^{g}$	275.7(3)	$F(2)\cdots O(5)^{h}$	281.7(3)
$F(6)\cdots O(6)$	279.8(3)		
$O(5)\cdots N(2)$	275.6(4)	$O(6)\cdots N(1)^{c}$	268.3(4)

Symmetry transformations used to generate equivalent atoms: *a* $-x+\frac{1}{2}, y-\frac{1}{2}, -z+\frac{1}{2}$; *b* $-x+\frac{1}{2}, y+\frac{1}{2}, -z+\frac{1}{2}$; *c* $x+1, y, z$; *d* $x-1, y, z$; *e* $-x, y-\frac{1}{2}, -z$; *f* $-x+1, y+\frac{1}{2}, -z$; *g* $-x+1, y-\frac{1}{2}, -z$; *h* $-x+1, y+\frac{1}{2}, -z$.

1597vs, 1472s, 1314m, 774vs, for compound **1**; 3400s (br), 1607vs, 1421s, 1087s, 829vs, for compound **2**. Magnetic susceptibilities of compound **1** were measured between 10 and 300 K using a Manics D5M5 susceptometer.

Results and Discussion

We were able to synthesize **1** and **2** from hydrofluoric acid solutions. Although, some related complexes have been prepared: $[MnCl_3(H_2O)B]$,[11] $[MnF_3(H_2O)(phen)]$,[11] $[MnF_3(H_2O)\{NH_2C(O)NH_2\}]\cdot 3H_2O$ and $[MnF_3(H_2O)B]\cdot 2H_2O$[12] [where B = 2,2′-bipy or 1,10-phenanthroline (phen)], no crystal structures have been reported.

Structural description of $[MnF_3(H_2O)(2,2'\text{-bipy})]$

In compound **1**, the organic base 2,2′-bipy acts as a bidentate ligand, (Fig. 1). No water molecules of crystallization were detected from the diffraction analysis. The manganese environment corresponds to a highly distorted octahedron with three short Mn–F distances (183.9, 183.5 and 183.5 pm), an intermediate Mn–N(2) distance (207.5 pm) and two long distances, Mn–O(1) (216.4 pm) and Mn–N(1) (221.5 pm) (Table 1). This strong distortion is due to both the Jahn–Teller effect inherent in the high-spin d^4 Mn^{III} ion and to the steric restrictions imposed by the chelate ligand with two nitrogen atoms in the *cis* position. In hydrated Mn^{III} fluorides with one or more water molecules bound to the metal, the octahedral distortion associated with the Jahn–Teller effect generally exhibits a strong elongation along the direction of the Mn–O water bond.[8,5] These different Mn–N distances for the same 2,2′-bipy ligand have been also found for di-μ-oxo-tetrakis(2,2′-bipyridine)-dimanganese(III, IV) perchlorate trihydrate,[19] where two 2,2′-bipy ligands are bound to one manganese(III) atom (Mn–N 213, 223; 213, 221 pm). On the other, the Mn–N(2) distance (207.5 pm) may seem unusually long; however, it is close to the published values for Mn–N (205 pm) in $[MnCl_3(2,2'\text{-bipy})]$,[20] where manganese(III) is also found in a six-fold co-ordination environment. In **1** the elongation is along the N(1)–Mn–O(1) axis, which is consistent with the directional preferences of the Jahn–Teller effect.

The Mn–F distances in **1** roughly coincide with the 'short' equatorial Mn–F distances found in other fluoromanganese(III) complexes, which are shortened by the Jahn–Teller effect.[1–8] The octahedra are slightly distorted around the central manganese atom (see X–Mn–X angles in Table 1). The angular displacements from linearity are produced by the steric hindrance

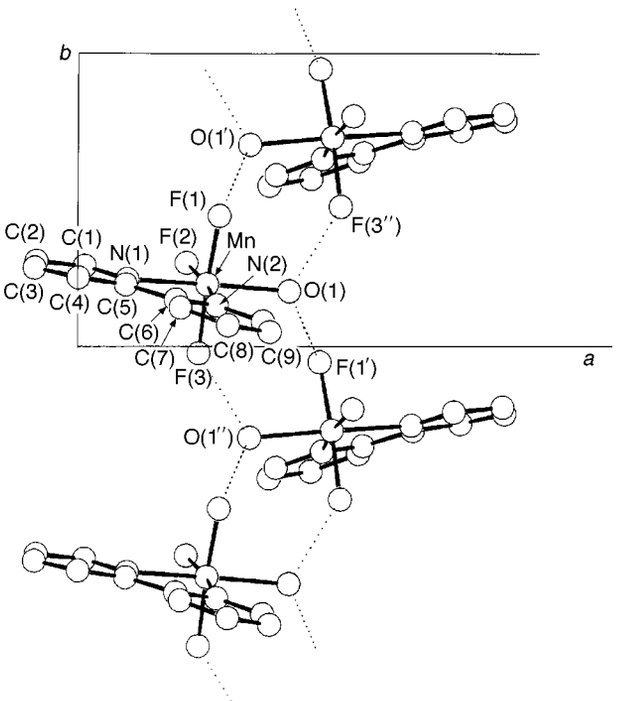

Fig. 1 A packing arrangement for $[MnF_3(H_2O)(2,2'\text{-bipy})]$ showing the intrachain hydrogen-bond connectivity. The hydrogen bonds are indicated by dotted lines. The C(10) label is omitted for clarity. Symmetry operations: $'-x+0.5, y+0.5, -z+0.5$ and $''-x+0.5, y-0.5, -z+0.5$

introduced by the pseudo-rigid 2,2′-bipy ligand in the complex $[MnF_3(H_2O)(2,2'\text{-bipy})]$. The N(1)–Mn–N(2) 'bite' angle of 76.0(1)° for 2,2′-bipy may be considered normal when compared with an average angle of 77° quoted in the literature.[21]

The $[MnF_3(H_2O)(2,2'\text{-bipy})]$ octahedra are packed in such a way that the long axis [N(1)–Mn–O(1)] is approximately perpendicular (94°) to the *b* axis. The planar ligands are stacked along this crystallographic direction in a zigzag fashion (Fig. 1). A detailed analysis of this structure shows a rich hydrogen-bonded framework which gives rise to octahedral chains, Fig. 1.

Structural description of 4,4′-bipy$H_2[MnF_4(H_2O)_2]\cdot 2H_2O$ 2

In compound **2** $[4,4'\text{-bipy}H_2]^{2+}$ merely acts as the charge-balancing cation. In the unit cell of **2** there are two non-equivalent octahedra (type A and type B) which are highly distorted by the Jahn–Teller effect (Fig. 2 and Table 1). The two water molecules co-ordinated to the metal occupy the axial positions of the octahedron, which correspond to the longer Mn–O (water) (219–226 pm) distances. In both types of octahedra the F–Mn–F and O–Mn–O angles are close to linear, with only very slight angular displacements (<3°), as can be seen in Table 1. The long axes (O–Mn–O) of the $[MnF_4(H_2O)_2]$ octahedra and the crystallographic *b* axis form angles of 46.2 and 44.8° for octahedra A and B, respectively.

Compound **2** contains a very extensive network of hydrogen bonds (Table 2 and Fig. 2). Thus, two kinds of anionic chains are observed parallel to the *a* axis: one is formed by type-A octahedra and the other by linked type-B octahedra. The water molecules of crystallization and the counter ions $[4,4'\text{-bipy}H_2]^{2+}$ are located among the chains (Fig. 2).

Magnetic properties

The magnetic susceptibility was measured only for compound **1** at temperatures ranging from 10 to 300 K. A Curie law behavior is observed over the entire temperature range. This behavior is expected for such a structure since the paramagnetic centers are too far away to show significant magnetic interactions above

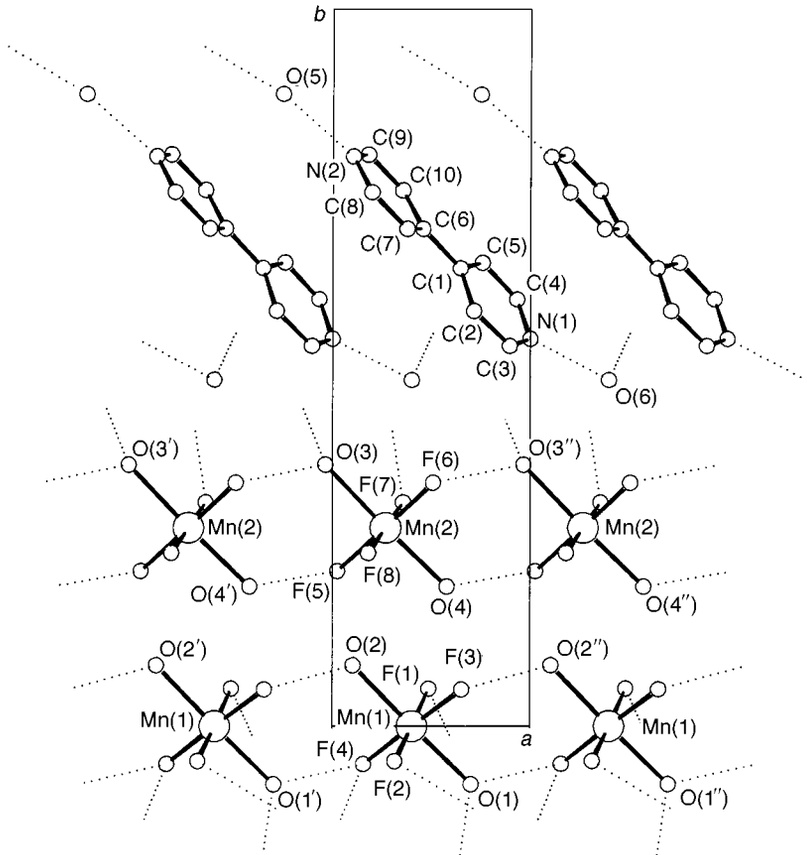

Fig. 2 A packing arrangement of 4,4′-bipyH$_2$[MnF$_4$(H$_2$O)$_2$]·2H$_2$O showing the equivalent octahedra associated into chains *via* hydrogen bonds. The hydrogen bonds are indicated by dotted lines. Symmetry operations: ′ $x + 1, y, z$ and ″ $x - 1, y, z$

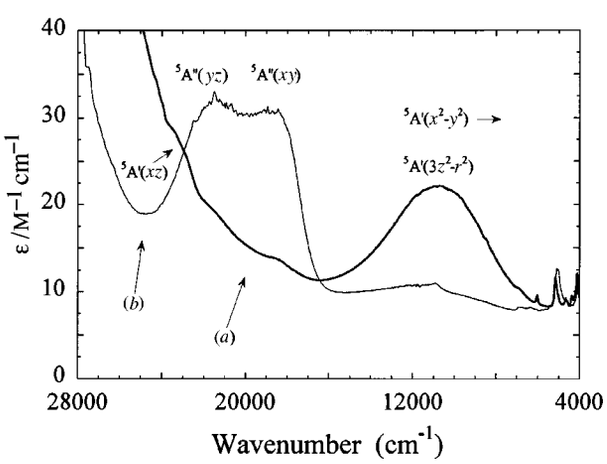

Fig. 3 Polarized optical absorption spectra of [MnF$_3$(H$_2$O)(2,2′-bipy)] taken with (*a*) *E* parallel to the monoclinic *a* and (*b*) parallel to the monoclinic *b* directions

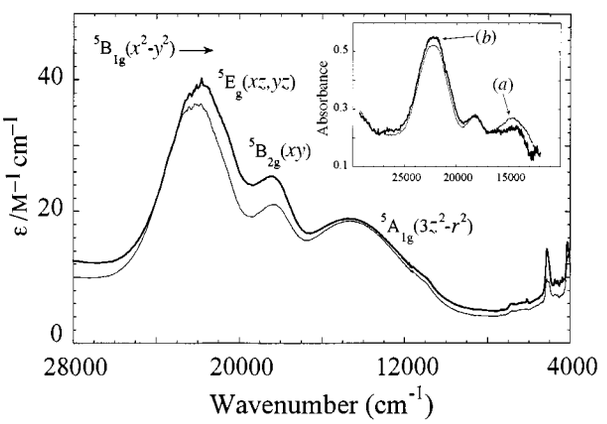

Fig. 4 Polarized optical absorption spectra of 4,4′-bipyH$_2$[MnF$_4$(H$_2$O)$_2$]$_2$·2H$_2$O along two oblique extinction directions. The inset depicts the polarized spectra of a needle-like crystal (400 × 90 × 30 μm) showing parallel extinctions with the crystallographic *a* axis. For comparison purposes, a constant absorption background of 0.25 has been subtracted from the *a* spectrum of the inset

10 K. The effective magnetic moment derived from the experimental Curie constant is $\mu_{eff} = 2.828(\chi T)^{\frac{1}{2}} = 4.55\ \mu_B$. This value is slightly smaller than that obtained for [MnF$_3$(H$_2$O)(2,2′-bipy)]. The magnetic moment obtained for compound **1** is somewhat lower than the spin-only magnetic moment for a high-spin d^4 configuration ground state (4.9 μ_B) with an isotropic gyromagnetic value of 2. However, the orbital contributions, which are negative for d^n cations with $n < 5$, could account slightly for such a deviation.

Electronic spectra

Manganese(III) compounds very often show a marked dichroism due to the low symmetry displayed by the manganese coordination polyhedron.[22] These effects are particularly intense in some fluoride crystals containing D_{4h} distorted [MnF$_6$]$^{3-}$ units.[6,7] The highly polarized $^5B_{1g} \longrightarrow {}^5A_{1g}$ broad band occurring at around ≈15 000 cm^{-1} is mainly responsible for the color change when the polarization plane of the light is rotated 90° around one of the equatorial F–Mn–F axes. Figs. 3 and 4 show the polarized optical absorption spectra of compounds **1** and **2**, respectively. For compound **1**, the spectra were taken with *E* parallel to the monoclinic *a* (σ) and *b* (π) directions. The π and σ symbols are employed here to emphasize that the spectra are taken parallel and perpendicular to the F(1)–Mn–F(3) bonds of the complex, respectively. For the crystal containing [MnF$_4$(H$_2$O)$_2$] units (compound **2**), the spectra were taken

along the two oblique extinction directions of a needle-shaped crystal. The spectra shown in the inset of Fig. 4 were obtained from a selected small crystal ($400 \times 90 \times 30$ μm^3) whose extinction directions were parallel and perpendicular to the needle axis; *i.e.* *a* and *b* crystallographic directions, respectively. These latter spectra were recorded by means of a special spectrophotometer for working with microsamples.[23] Unlike compound **1**, the crystals of compound **2** exhibited a low dichroism which is illustrated in Fig. 4. This behavior is due to the almost orthogonal orientations displayed by the axial O–Mn–O bonds of those $[MnF_4(H_2O)_2]$ complexes which are connected with each other through the 2_1 screw axis parallel to *b*. A similar situation has also been found in $TlMnF_4$ whose optical spectra are isotropic within the basal plane by the antiferrodistortive structure of the $[MnF_{\frac{4}{2}}F_2]$ octahedra.[5,6,24]

The spectra consist of several broad bands in the range 8000–26 000 cm^{-1} which are strongly polarized for compound **1** and weakly polarized for compound **2**. The values of the molar absorption coefficients measured at the band maxima are characteristic of spin-allowed crystal field transitions within the 3d^4 configuration.[25]

Compound 1. The optical spectra of compound **1** are somewhat different from those of compound **2**. The band assignment is made on the basis of a $[MnF_3(H_2O)(2,2'\text{-bipy})]$ complex, displaying a nearly C_s symmetry with the mirror plane almost perpendicular to the F(1)–Mn–F(3) direction (Fig. 1). The different Mn–N distances [222 and 208 pm for Mn–N(1) and Mn–N(2), respectively] indicate that the unoccupied Mn d orbital must lie on the equatorial plane of the complex defined by the Mn–F(3) and Mn–N(2) directions. In order to assign the spectral transitions and by analogy with other octahedral elongated Mn^{III} complexes, the local site symmetry was defined with the longer axis [N(1)–Mn–O(1)] as the local *z* axis; whereas the local *x* and *y* axes point along the F(2)–Mn–N(2) and F(1)–Mn–F(3) directions, respectively. Thus the d_z^2 orbital, which is half filled, points along the N(1)–Mn–O(1) axis while the unoccupied $d_{x^2-y^2}$ orbital of highest energy points along the F(1)–Mn–F(3) and F(2)–Mn–N(2) ones. This results in a transformation of the typical C_s axes such that now the *y* axis is almost perpendicular to the mirror plane of the C_s point group. Therefore, the local *y* direction now transforms as A″, while the local *x* and *z* directions transform as A′.

Within C_s there are four possible spin and parity allowed electric dipole d–d transitions from the ground state, $^5A'(x^2 - y^2)$, to excited states of either $^5A''$ or $^5A'$ symmetry depending on whether the light polarization is directed along the axial F(1)–Mn–F(3) bond (*y* direction) or lies on the (*x*, *z*) symmetry plane, respectively (Fig. 5). The first broad band at 11 000 cm^{-1} which corresponds to the $^5A'(x^2 - y^2) \longrightarrow {}^5A'(z^2)$ transition, is highly polarized and absorbs almost exclusively (90%) along *a* (*x*,*z*-polarized band) (Fig. 5). The presence of this band (10% intensity) in the spectrum polarized along the crystallographic *b* axis is due to a slight distortion of the axial F(1)–Mn–F(3) direction from the monoclinic *b* direction (19°). The two bands at 18 500 and 21 500 cm^{-1} observed in the π(*b*) spectrum (Fig. 3) are *y* polarized and therefore must be associated with $^5A' \longrightarrow {}^5A''$ electronic transitions. These bands are still observed as small shoulders in the σ spectrum parallel to *a*. Interestingly, the σ spectrum also shows another shoulder, not observed in π polarization around 23 000 cm^{-1} which probably corresponds to the $^5A'(x^2 - y^2) \longrightarrow {}^5A'(xz)$ transition. Given that this band is largely masked by the tail of the ligand-to-metal charge transfer band associated with the N ligands, no conclusive assignment for this shoulder can be made from the electronic spectrum. It must be pointed out, however, that the one-electron d_{xz} orbital is expected to be the lowest lying Mn^{III} level since the π-bonding interactions of the N ligands essentially exert no influence on its energy [$e_\pi(N) = 0$].[25] In fact, while the one-electron d_{xz} energy depends on the two π-bonding O(1) and F(2) ligands, the energies of the corresponding d_{yz} and d_{xy} levels contain π-bonding contributions from three ligands: F(1) and F(3) ligands located in the *y* axis, and the O(1) or the F(2) ligands for the d_{yz} and d_{xy} levels respectively. The reason for the slightly higher energy of the $^5A''(yz)$ compared to $^5A''(xy)$ may be seen in the weaker π bonds along *z* due to the rather long spacing in this direction.

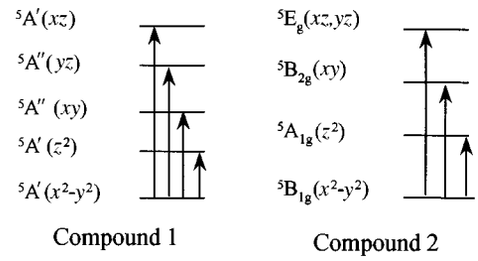

Fig. 5 State diagram showing the electronic transitions for compounds **1** and **2** on the basis of C_s and D_{4h} point groups, respectively

Compound 2. The spectrum of compound **2** which is associated with the $[MnF_4(H_2O)_2]$ complex, is very similar to those observed in other Mn^{III} fluoride complexes, *e.g.* $[MnF_6]$,[6,7] and consequently its assignment can easily be made on the basis of these D_{4h} symmetry complexes but replacing the axial F ligands by the oxygen of water molecules. The three bands observed at $\varepsilon_1 = 14\,600$, $\varepsilon_2 = 18\,400$ and $\varepsilon_3 = 22\,000$ cm^{-1}, are assigned to the spin allowed intraconfigurational d^4 transitions as indicated in Fig. 4. Here the *z* axis is taken along the axial O–Mn–O line. Values of the equatorial ligand field parameter, $10Dq(\text{eq}) = \varepsilon_2 = 18\,400$ cm^{-1} and the tetragonal splitting of the parent octahedral ^5E_g and $^5T_{2g}$ states, $\Delta_e = \varepsilon_1 = 14\,600$ cm^{-1} and $\Delta_t = \varepsilon_3 - \varepsilon_2 = 3600$ cm^{-1}, respectively, are derived from the spectra of Fig. 4. It is interesting to note that although the ratio $\Delta_e/\Delta_t = 4$ coincides with that measured for the whole series of Mn^{III} fluorides (see Table 1 of ref. 6), the values of the spectroscopic parameters Δ_e and Δ_t, however, are similar only to those found for the $AMnF_4$ (A = K, Rb, Cs, Tl) family, whose $[MnF_{\frac{4}{2}}F_2]$ units exhibit the highest tetragonal distortion of the Mn^{III} fluoride series: *i.e.* $x_D = R_{ax}/R_{eq} - 1 = 0.17$ ($R_{eq} = 184$, $R_{ax} = 215$ pm).[6] Nevertheless it must be observed that while the average equatorial Mn–F distance, $R_{eq} = 184$ pm, is the same for the $[MnF_6]$ complexes and $[MnF_4(H_2O)_2]$ studied here, the axial Mn–O bond distance, R_{ax} (O) = 223 pm, is significantly longer than the axial Mn–F distance for $AMnF_4$, $R_{ax} = 215$ pm, and therefore the corresponding tetragonal distortion parameter for compound **2** is $x_D = 0.21$. The fact that Δ_e and Δ_t are similar despite the longer Mn–O axial distance, must be ascribed to the presence of axial water molecules. In fact we can compare the ligand field effects of F^- and H_2O for the same axial bond distance taking into account the optical and structural correlations established in ref. 6 for the whole fluoride series. From the empirical relations[6] $\Delta_e = 8.8 \times 10^4\, x_D$ and $\Delta_t = 2.2 \times 10^4\, x_D$ (in cm^{-1}), we obtain values of $\Delta_e = 18\,500$ cm^{-1} and $\Delta_t = 4600$ cm^{-1} corresponding to a $[MnF_6]^{3-}$ complex with $R_{eq} = 184$ pm and $R_{ax} = 223$ pm {the same distances as those for the present $[MnF_4(H_2O)_2]$ complex}. Therefore, the differences between the Δ_e and Δ_t values obtained for $[MnF_4(H_2O)_2]$ and $[MnF_6]$, $\delta(\Delta_e) = 3900$ cm^{-1} and $\delta(\Delta_t) = 1000$ cm^{-1}, must be associated with the stronger ligand field strength of the water molecules. This noteworthy result allows us to compare quantitatively the spectroscopic bonding parameters e_σ and e_π of F^- and H_2O.‡ In particular we obtain values of $e_\sigma(H_2O) - e_\sigma(F) = 2000$ cm^{-1} and $e_\pi(H_2O) - e_\pi(F) = 500$ cm^{-1} for $R_{ax} = 223$ pm, thus con-

‡ Within an atomic angular overlap model the Δ_e and Δ_t, parameters are given by $2[e_\sigma(L) - e_\sigma(z)]$ and $2[e_\pi(L) - e_\pi(z)]$, respectively, where L and z represent the equatorial and axial ligands.[25] For two complexes $[MnX_4Y_2]$ and $[MnX_6]$ with equal R_{ax} and R_{eq} distances, the parameters are $\delta(\Delta_e)/2 = e_\sigma(Y) - e_\sigma(X)$ and $\delta(\Delta_t)/2 = e_\pi(Y) - e_\pi(X)$.

firming that the σ- and π-axial interactions of the oxygen are higher than those of the fluorine following the trends of the spectrochemical series.[25]

Sharp features observed between 4000 and 6000 cm^{-1} in the spectra of compound **1** (Fig. 3) and compound **2** (Fig. 4) are due to overtones of the hydrogen vibrations of the water molecules and the C–H bonds of the bipy molecules according to Rodriguez *et al.*[6]

Acknowledgements

The authors wish to thank Professor H. zur Loye (Cambridge, MA, USA) for a critical reading of the manuscript. P. N. and J. F. wish to acknowledge the late Professor Maria Soledad Palacios' many fruitful discussions about this paper.

References

1 P. Núñez, J. Darriet, P. Bukovec, A. Tressaud and P. Hagenmuller, *Mater. Res. Bull.*, 1987, **22**, 661.
2 P. Núñez, A. Tressaud, J. Darriet, P. Hagenmuller, G. Hahn, G. Frenzen, W. Massa, D. Babel, A. Boireau and J. L. Soubeyroux, *Inorg. Chem.*, 1992, **31**, 770.
3 P. Núñez, J. Darriet, A. Tressaud, P. Hagenmuller, S. Kumer, W. Massa and D. Babel, *J. Solid State Chem.*, 1988, **77**, 240.
4 P. Núñez, A. Tressaud, W. Massa, D. Babel, A. Boireau and J. L. Soubeyroux, *Phys. Status Solidi A*, 1991, **127**, 505.
5 P. Núñez, A. Tressaud, J. Grannec, P. Hagenmuller, G. Hahn, G. Frenzen, W. Massa, D. Babel, A. Boireau and J. L. Soubeyroux, *Z. Anorg. Allg. Chem.*, 1992, **609**, 71.
6 F. Rodríguez, P. Núñez and M. C. Marco de Lucas, *J. Solid State Chem.*, 1994, **110**, 370.
7 P. Núñez, F. Rodríguez and M. C. Marco de Lucas, *Adv. Mater. Res.* (*Zug*, *Switz.*), 1994, **1**, 447.
8 W. Massa and D. Babel, *Chem. Rev.*, 1988, **88**, 275.
9 F. Palacio and M. C. Morón, in *Research Frontiers in Magnetochemistry*, ed. C. J. O'Connor, World Scientific, 1993, p. 227.
10 U. Bentrup, L. Schröder and W. Massa, *Z. Naturforsch.*, *Teil B*, 1992, **47**, 789.
11 M. N. Bhattacharjee, M. K. Chaudhuri and R. N. D. Purkayastha, *Inorg. Chem.*, 1989, **28**, 3747.
12 H. A. Goodwin and R. N. Sylva, *Aust. J. Chem.*, 1967, **20**, 629; 1965, **18**, 1743.
13 M. N. Bhattacharjee, M. K. Chaudhuri and R. N. D. Purkayastha, *Inorg. Chem.*, 1985, **24**, 447; *Polyhedron*, 1985, **4**, 621.
14 T. E. Moore, E. Ellis and P. E. Selwood, *J. Am. Chem. Soc.*, 1952, **72**, 856.
15 *International Tables for Crystallography*, ed. A. J. C. Wilson, Kluwer Academic Publishers, Dordrecht, 1992, vol. C, Table 6.1.1.4, pp. 500–502, Table 4.2.6.8 pp. 219–222 and Table 4.2.4.2, pp. 193–199.
16 G. M. Sheldrick, SHELXS 86, Program for Crystal Structure Determination, *Acta Crystallogr.*, *Sect. A*, 1990, **46**, 467.
17 G. M. Sheldrick, SHELXL 93, Program for Crystal Structure Refinement, University of Göttingen, 1993.
18 N. E. Brese and M. O'Keefe, *Acta Crystallogr.*, *Sect. B*, 1991, **47**, 192 and refs. therein.
19 P. M. Plaskin, R. C. Stoufer, M. Mathew and G. J. Palenik, *J. Am. Chem. Soc.*, 1972, **94**, 2121.
20 S. P. Perlepes, A. G. Blackman, J. C. Huffman and G. Christon, *Inorg. Chem.*, 1991, **30**, 1665.
21 W. Fitzgerald and B. J. Hathaway, *J. Chem. Soc.*, *Dalton Trans.*, 1981, 567.
22 T. S. Davis, J. P. Fackler and M. J. Weeks, *Inorg. Chem.*, 1968, **7**, 1994.
23 B. A. Moral and F. Rodríguez, *Rev. Sci. Instrum.*, 1995, **66**, 5176.
24 P. Kohler, W. Massa, D. Reinen, B. Hofmann and R. Hoppe, *Z. Anorg. Allg. Chem.*, 1978, **446**, 131.
25 See, A. B. P. Lever, *Inorganic electronic spectroscopy*, Elsevier, Amsterdam, 1984, pp. 53–69 and 763.

Received 20*th June* 1997; *Paper* 7/04368F